Equation 17 follows upon taking the derivative and using

$$\frac{\partial}{\partial x}\,\mathrm{erf}\,(x^{1/2}) = \frac{1}{(\pi x)^{1/2}}e^{-x}$$

Equation 18 for $F_2(x)$ is obtained in a similar manner.

Now we proceed to derive eq 19 for $F_3(x)$. First we rearrange the sum in eq A.14 in the form

$$F_3(x) = \frac{1}{4}e^{-x}\sum_{m=0}^{\infty}\frac{2^{m+1}x^{m-1}}{(2m+1)!!}(m-1)m(2m-1) \qquad \text{(A.20)}$$

Next we write $(m-1)m(2m-1) = 2(m-{}^3/_2)(m-{}^1/_2)(m+{}^1/_2) + {}^3/_2m - {}^3/_4$ and decompose $F_3(x)$ into three terms

$$F_3(x) = {}^1\!/_4e^{-x}(F_3^{(1)}(x) + F_3^{(2)}(x) + F_3^{(3)}(x)) \qquad \text{(A.21)}$$

where

$$F_3^{(1)}(x) = 2\sum_{m=0}^{\infty}\frac{2^{m+1}x^{m-1}}{(2m+1)!!}(m-{}^3\!/_2)(m-{}^1\!/_2)(m+{}^1\!/_2) = 4x^{3/2}\frac{\partial^3}{\partial x^3}\sum_{m=0}^{\infty}\frac{2^m x^{m+1/2}}{(2m+1)!!} = 2\pi^{1/2}x^{3/2}\frac{\partial^3}{\partial x^3}[e^x\,\mathrm{erf}\,(x^{1/2})] \qquad \text{(A.22)}$$

$$F_3^{(2)}(x) = (2)\frac{3}{2}\sum_{m=0}^{\infty}\frac{2^m x^{m-1}}{(2m+1)!!}m = \frac{3}{2}\pi^{1/2}\frac{\partial}{\partial x}[x^{-1/2}e^x\,\mathrm{erf}\,(x^{1/2})] \qquad \text{(A.23)}$$

$$F_3^{(3)}(x) = -\frac{3}{2}\sum_{m=0}^{\infty}\frac{2^m x^{m-1}}{(2m+1)!!} = -\frac{3}{4}\pi^{1/2}x^{-3/2}e^x\,\mathrm{erf}\,(x^{1/2}) \qquad \text{(A.24)}$$

Taking the derivatives and combining the above expressions gives $F_3(x)$ (eq 19). The expression for $F_4(x)$ (eq 20) is derived by using the same method (however, in this case care must be taken to subtract the nonvanishing $m = 0$ term following the change of variables $m \rightarrow m + 1$ in the m sum).

References and Notes

(1) H. Yamakawa, "Modern Theory of Polymer Solutions", Harper and Row, New York, 1971, and references therein.
(2) A. Peterlin, *J. Chem. Phys.*, **33**, 1799 (1960).
(3) A. Peterlin, *Pure Appl. Chem.*, **12**, 563 (1966).
(4) P. Pincus, *Macromolecules*, **10**, 210 (1977).
(5) P. Pincus, *Macromolecules*, **9**, 386 (1976).
(6) D. P. Pope and A. Keller, *Colloid. Polym. Sci.*, **256**, 751 (1978).
(7) C. J. Farrell, A. Keller, M. J. Miles, and D. P. Pope, *Polymer*, **21**, 1292 (1980).
(8) A. Keller and J. A. Odell, *Colloid Polym. Sci.*, in press.
(9) P. J. Flory, "Statistical Mechanics of Chain Molecules", Interscience, New York, 1969.
(10) R. B. Bird, O. Hassager, R. C. Armstrong, and C. F. Curtiss, "Dynamics of Polymeric Liquids", Vol. I and II, Wiley, New York, 1977.
(11) P. G. DeGennes, "Scaling Concepts in Polymer Physics", Cornell University Press, Ithaca, NY, 1979.
(12) P. E. Rouse, *J. Chem. Phys.*, **21**, 1972 (1953).
(13) B. H. Zimm, *J. Chem. Phys.*, **24**, 269 (1956).
(14) K. Nagai, *J. Chem. Phys.*, **40**, 2818 (1964).
(15) The exact partition function can be computed analytically.[9] For consistency, we keep only terms compatible with the lowest order correction in the $1/n$ expansion of the distribution function.
(16) This is no longer true for extremely strong tensile force such that $a \gg \xi$. However, both the $1/n$ expansion of the distribution function and the linear mode analysis become invalid in this regime. We have plotted the freely jointed chain results only in the region where we expect the approximations involved in eq 8, 11, and 12 to be valid.
(17) J. L. Lumley, *J. Polym. Sci., Macromol. Rev.*, **7**, 263 (1973).
(18) Y. Rabin, *J. Polym. Sci., Polym. Lett.*, **23**, 11 (1985).
(19) M. Abramowitz and L. A. Stegun, Eds., "Handbook of Mathematical Functions", National Bureau of Standards Applied Mathematics Series, USGPO, Washington, DC, 1970.

Molecular Dimensions in Poly(ethylene terephthalate) by Small-Angle Neutron Scattering

K. P. McAlea and J. M. Schultz*

Department of Chemical Engineering, University of Delaware, Newark, Delaware 19716

K. H. Gardner

Experimental Station, E. I. du Pont de Nemours and Company,
Wilmington, Delaware 19898

G. D. Wignall

National Center for Small Angle Scattering Research, Oak Ridge National Laboratory, Oak Ridge, Tennessee 37830.

Received May 22, 1984

ABSTRACT: Single-chain dimensions measured in bulk poly(ethylene terephthalate) (PET) samples by small-angle neutron scattering (SANS) have been found to be close to the unperturbed value. Thin films with labeled (deuterated) PET concentrations as high as 40% were cast from solution. Measurements were made with two molecular weight materials at three sample–detector distances. The SANS molecular weights obtained from both Zimm and Debye fits are within 25% of the GPC values in all cases. The average value of $R_g^w/M_w^{1/2}$ is 0.373 compared to the theoretical value for unperturbed dimensions of 0.394.

Introduction

The dimensions of chain molecules in amorphous polymers have been investigated by small-angle neutron scattering in a wide range of systems in the past decade and in general have been shown to be close to the unperturbed dimensions of chains in ideal Θ-solvents.[1-9] However, despite the importance of poly(ethylene terephthalate) (PET) from both scientific and technological viewpoints, to our knowledge no measurements of chain dimensions have been reported in either the amorphous or crystalline states. This is partly due to the difficulties encountered in preparing samples in which the background scattering arising from the polymer matrix and heterogeneities (voids, catalyst/solvent residues, etc.) is sufficiently low so as not to mask the scattering due to the contrast between the labeled (deuterated) and unlabeled (hydrogenous) molecules. Moreover, many of the earlier experiments[1-6] were performed with low relative concentra-

0024-9297/85/2218-0447$01.50/0

Table I
GPC Molecular Weights

	M_n	M_w	M_z	M_w/M_n
PET-D[a]				
series A	34 500	103 600	204 500	3.01
series B	27 400	84 700	192 800	3.09
PET-H	28 900	89 800	189 000	3.11

[a] Values for the PET-D molecules are corrected for the difference (1.042) in mass between PET-D and PET-H repeat units.

tions of labeled molecules which intensified the problem of background subtraction.[10] In this communication we wish to report measurements of molecular dimensions in PET from samples where the background scattering has been reduced to an acceptably small fraction of the scattering due to the labeled molecules. This has been accomplished by improvements in the sample preparation technique to reduce the concentration of heterogeneities giving rise to background scattering and also by use of high concentrations of labeled polymer. It has been shown earlier that both the radius of gyration and the molecular weight can be obtained from a single concentration measurement, provided the molecular weights of the labeled and unlabeled molecules are matched.[11]

Sample Preparation and Characterization

Fully deuterated PET with M_w = 32600 was supplied by Allied Chemical Co. This material was solid-state polymerized under vacuum at 240 °C for 50 (series A) and 40 (series B) h to obtain high molecular weight polymer. The hydrogenous material was commercial PET (Goodyear Cleartuff, Lot 1002A). The three materials were characterized by GPC as is shown in Table I.

Protonated blanks, deuterated blanks, 20 wt % (volume fraction = 0.193) PET-D, and 40 wt % (volume fraction = 0.390) PET-D samples were prepared. Sample material was first dissolved in trifluoroacetic acid (TFA) (1 g in 100 mL of solution) at room temperature and then reprecipitated by slowly pouring the solution into a blender containing ice water. The polymer was then filtered, washed with water and acetone, and dried under vacuum at 100 °C for 24 h. A small amount (0.5 g) of the dried polymer flakes was then redissolved in TFA in a petri dish and the solution slowly evaporated at 60 °C on a hot plate. When the solution reached the consistency of a gel, the dish was quickly immersed in water, yielding a cloudy polymer film. The films were dried under vacuum for 48 h and then pressed at 10 000 psi at 100 °C for 15 min. Our experience has shown that this pressing step considerably reduces the coherent scattering in the protonated and deuterated blanks presumably by eliminating voids in the samples.

The as-prepared films are semicrystalline by WAXS and density measurements show them to be 30% crystalline on the average.

Experimental Section

The neutron measurements were performed at The National Center for Small Angle Scattering Research (Oak Ridge National Laboratory) both on the NSF-funded 30-m SANS facility[12] at the High Flux Isotope Reactor (HFIR) and also on the 10-m SANS instrument located at the Oak Ridge Research Reactor (ORR). For the 30-m SANS facility, the area detector (64 × 64 cm^2), with 1-cm^2 element size, was mounted on rails inside a 20-m vacuum flight path and was positioned at sample-to-detector distances of 12.0 and 18.9 m. For the 10-m SANS instrument an identical detector is positioned at a fixed sample-to-detector distance of 4.5 m, and thus the measurements on the two different instruments sampled different ranges of the scattering vector $\mathbf{Q} = 4\pi\lambda^{-1} \sin\theta$, giving an overall range of $0.004 < Q < 0.125$ Å^{-1} where λ = 4.75 Å is the incident wavelength and 2θ is the angle of scatter. In all three Q ranges the scattering patterns were corrected on a cell-by-cell basis for instrumental backgrounds, detector efficiency variation, divided by the sample transmission (T) and thickness and normalized to a constant incident flux. Correction for the spatial variation of detector efficiency was accomplished by dividing all measured scattering patterns by the background-corrected scattering from an isotropic scatterer (water or polyethylene). Blank samples of pure PET-D and PET-H were also measured in all three Q ranges to check for the presence of scattering from voids or other heterogeneities and to provide a basis for subtraction of the angular-independent incoherent scattering arising principally from ^{1}H nuclei.

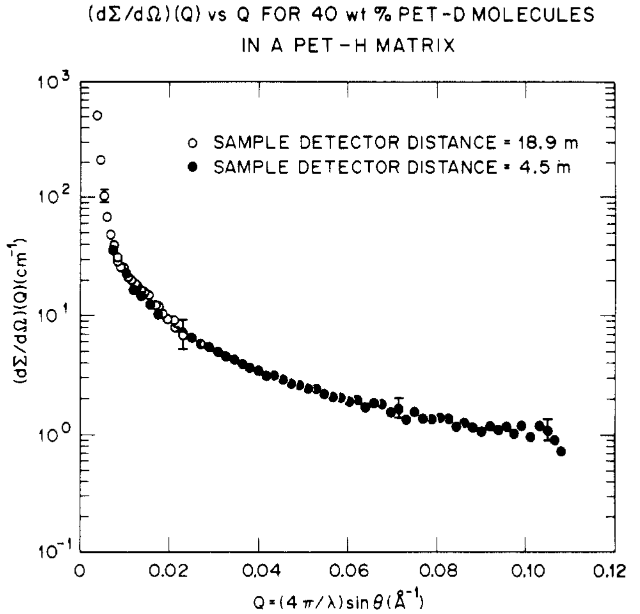

Figure 1. (dΣ/dΩ)(Q) vs. Q for a sample containing 40 wt % PET-D (M_w = 84700) in a PET-H matrix (M_w = 89800), measured in two angular ranges; (○) SDD, 18.9 m; (●) SDD, 4.5 m.

The corrected scattering patterns all exhibited cylindrical symmetry about the incident beam and the measured intensities were therefore radially averaged and converted to an absolute differential scattering cross section (dΣ/dΩ)(Q) per unit solid angle per unit volume of material (in units of cm^{-1}) by comparison with the scattering of secondary standards of monodisperse polystyrenes[11] of known molecular weight and independently calibrated aluminum single crystals containing ~0.7% voids.[13] The overall agreement between all calibration standards was better than ±5% after scaling for the different sample–detector distances (SDD) used in each Q range.

Results and Discussion

Figure 1 shows the scattering cross section for a partially labeled blend containing 40 wt % PET-D in a PET-H matrix, measured in two different Q ranges. The overlap between data sets is reasonable, indicating that the consistency of the absolute calibration procedures is better than ±5%. Figure 2 shows the corresponding cross sections for an unlabeled PET-H sample. The scattering is very small compared to that from the labeled sample (Figure 1) and consists mainly of angle-independent incoherent scattering from ^{1}H nuclei. It is well-known that for predominantly hydrogenous matrices there is a considerable contribution due to multiple scattering and hence the results do not indicate a true cross section which is a material (intensive) property. However, even for samples showing appreciable multiple scattering, the pattern is still independent of angle. To a first approximation, the flat incoherent scattering is proportional to $1 - T$, where T is the transmission ratio, for partially labeled samples of bulk polymers[14] and water[15] for H/D ratios greater than 50%, and this scaling factor was used to estimate the incoherent

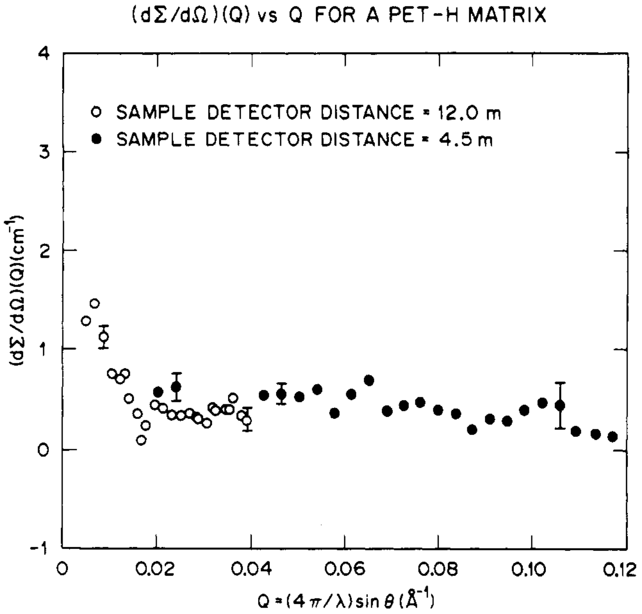

Figure 2. $(d\Sigma/d\Omega)(Q)$ vs. Q for a protonated blank (100% PET-H, $M_w = 89800$) measured in two angular ranges: (○) SDD, 18.9 m; (●) SDD, 4.5 m.

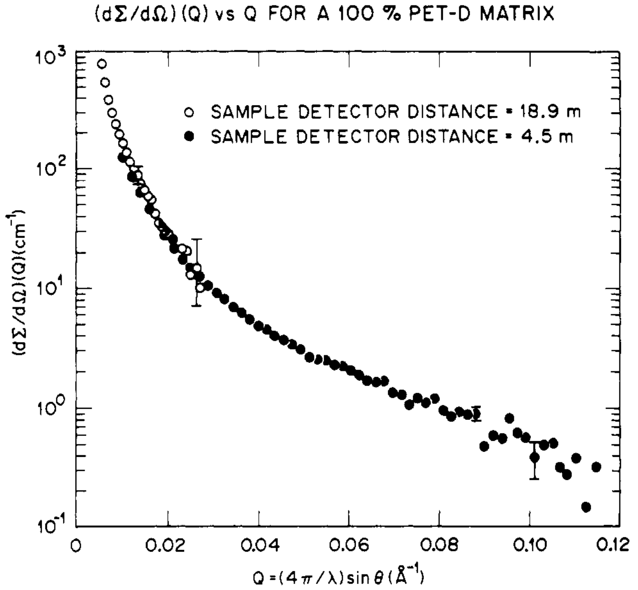

Figure 3. $(d\Sigma/d\Omega)(Q)$ vs. Q for a deuterated blank (100% PET-D, $M_w = 84700$) measured in two angular ranges: (○) SDD, 18.9 m; (●) SDD, 4.5 m.

background contribution to subtract from the data. The correction was very small for $Q < 0.025$ Å^{-1}.

Table II
Zimm and Debye Fit Values of R_g^z and M_w

		Zimm fit values		Debye fit values	
SDD, m	X	R_g^z, Å	$10^{-3}M_w$	R_g^z, Å	$10^{-3}M_w$
		Sample Series A (M_w (GPC) = 103.6×10^3)			
12.0	0.39	185.5[a]	128.0[a]	153.2[a]	115.0[a]
		n/a	n/a	143.6[b]	106.0[b]
		Sample Series B (M_w (GPC) = 84.7×10^3)			
18.0	0.39	131.7[a]	77.3[a]	136.6[a]	71.8[a]
		142.4[b]	86.0[b]	136.5[b]	80.3[b]
18.0	0.193	130.8[a]	87.3[a]	n/a	n/a
		125.8[b]	85.1[b]	148.6[b]	66.4[b]
5.0	0.39	159.7[a]	91.3[a]	n/a	n/a
		144.3[b]	86.9[b]	140.6[b]	107.4[b]
5.0	0.193	n/a	n/a	120.0,[a] 138.0[a]	75.8,[a] 86.9[a]
		152.8[b]	98.8[b]	133.2[b]	86.5[b]

[a] Values derived by assuming the background scattering heterogeneities are present in PET-H and PET-D. [b] Values derived by assuming the background scattering heterogeneities are present in PET-D only.

Figure 3 shows the cross section for a fully deuterated PET-D blank which exhibits considerable coherent scattering. It is to be expected that a fraction of this background will be present in the 20% and 40% labeled samples. Different methods for subtracting this component were tried, with the result that at 20% and 40% labeling level the coherent background contribution is sufficiently small that the chain dimensions and molecular weights derived from the data are independent of the method of subtraction (see Table II). As there is virtually no coherent scattering in the fully protonated blank, we believe that the background scattering arises from impurities in the deuterated polymer. An elemental analysis performed by X-ray fluorescence spectroscopy shows the presence of Si in the PET-D material. The source of this impurity is unknown; no purification scheme seems to eliminate it. The scattering contribution from an impurity (voids, catalyst/solvent residue) present in a polymer matrix may be written[16]

$$\frac{d\Sigma}{d\Omega}(Q) = N_p V_p^2(\rho - \rho_p)^2|F(Q)|^2 \tag{1}$$

where V_p is the impurity particle volume, N_p is the number of particles per unit volume, ρ_p is the scattering length density (SLD) of the impurity, ρ is the SLD of the polymer matrix, and $F(Q)$ is the form factor of the particles. For a 100% PET-D sample, eq 1 is

$$\left[\frac{d\Sigma}{d\Omega}(Q)\right]_{100\%\,\text{PET-D}} = N_p V_p^2(5.69 \times 10^{10} - \rho_p)^2|F(Q)|^2 \tag{2}$$

If we assume that N_p, V_p, and $F(Q)$ are independent of the labeled polymer concentration, then we may write the impurity scattering contribution in a partially labeled sample in terms of $[(d\Sigma/d\Omega)(Q)]_{100\%\,\text{PET-D}}$:

$$[(d\Sigma/d\Omega)(Q)] = \frac{(\rho - \rho_p)^2}{(5.69 \times 10^{10} - \rho_p)^2}\left[\frac{d\Sigma}{d\Omega}(Q)\right]_{100\%\,\text{PET-D}} \tag{3}$$

If we assume the impurity is present only in the PET-D, then the right-hand side of eq 3 must be multiplied by the volume fraction (X) of labeled polymer. The total coherent scattering cross section $[(d\Sigma/d\Omega)(Q)]_{\text{TOT}}$ with a given volume percent of labeled polymer is the sum of contributions due to the labeled molecules $[(d\Sigma/d\Omega)(Q)]_{\text{MOL-}X\%}$ and a background cross section given by eq 3. For samples containing 20 and 40 wt % PET-D molecules, the volume fractions of labeled polymer are 0.193 and 0.390 and the matrix scattering length densities (SLD) are 3.02×10^{10} and 3.69×10^{10} cm^{-2}, respectively. Thus, after subtraction of the incoherent backgrounds and assuming the impurity is present only in the PET-D, the scattering for the two partially labeled samples may be written

$$\left[\frac{d\Sigma}{d\Omega}(Q)\right]_{\text{TOT}(X=0.193)} = \left[\frac{d\Sigma}{d\Omega}(Q)\right]_{\text{MOL}(X=0.193)} + 0.193\frac{(3.02 \times 10^{10} - \rho_p)^2}{(5.69 \times 10^{10} - \rho_p)^2}\left[\frac{d\Sigma}{d_\omega}(Q)\right]_{100\%\,\text{PET-D}} \tag{4}$$

$$\left[\frac{d\Sigma}{d\Omega}(Q)\right]_{\text{TOT}(X=0.39)} = \left[\frac{d\Sigma}{d\Omega}(Q)\right]_{\text{MOL}(X=0.39)} + 0.39\frac{(3.69 \times 10^{10} - \rho_p)^2}{(5.69 \times 10^{10} - \rho_p)^2}\left[\frac{d\Sigma}{d\Omega}(Q)\right]_{100\%\,\text{PET-D}} \tag{5}$$

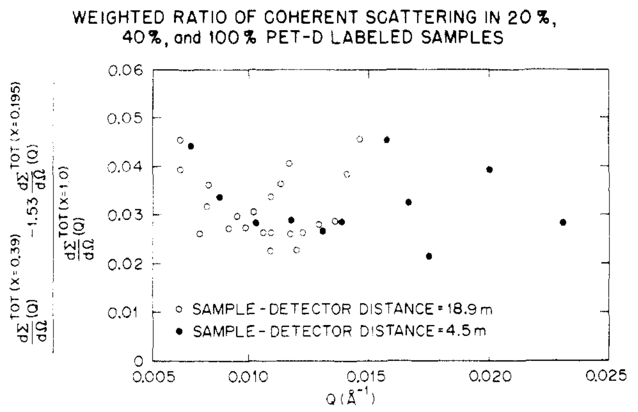

Figure 4. Left-hand side of eq 6 plotted against Q for data taken in two angular ranges: (○) SDD, 18.9 m; (●) SDD, 4.5 m (PET-D, M_w = 84700; PET-H, M_w = 89800).

As the molecular scattering cross sections $[(d\Sigma/d\Omega)\cdot(Q)]_{MOL-X\%}$ are proportional to $X(1-X)$, one can solve eq 4 and 5 for the unknown particle length density ρ_p. Substituting the known ratio of the molecular cross sections at 20 and 40 wt % labeling $([(d\Sigma/d\Omega)(Q)]_{MOL(X=0.39)} = 1.53[(d\Sigma/d\Omega)(Q)]_{MOL(X=0.193)})$, one may rearrange eq 4 and 5 to

$$\frac{\left[\frac{d\Sigma}{d\Omega}(Q)\right]_{TOT(X=0.39)} - 1.53\left[\frac{d\Sigma}{d\Omega}(Q)\right]_{TOT(X=0.193)}}{\frac{d\Sigma}{d\Omega}(Q)_{100\% PET\text{-}D}} = \left[\frac{0.39(3.67\times10^{10}-\rho_p)^2}{(5.69\times10^{10}-\rho_p)^2} - 1.53\times 0.193\frac{(3.01\times10^{10}-\rho_p)^2}{(5.69\times10^{10}-\rho_p)^2}\right] \quad (6)$$

This equation assumes that the background scattering arises from a single type of scattering heterogeneity with a given SLD and, if this is valid, then the left-hand side of eq 6 should be a constant, independent of Q. Figure 4 shows this ratio in the Q range $0.006 \leq Q < 0.025$ Å^{-1} where the data are most sensitive to the subtraction of the background scattering. The approximate constancy of this ratio indicates that the assumptions used are not unreasonable and from the average value of the ratio we calculate $\rho_p = 2.78 \times 10^{10}$ cm^{-2}. Alternatively if one assumes that the background heterogeneities are present in both H and D polymer, one should remove the concentration X from the second terms of eq 4 (X = 0.193) and 5 (X = 0.390). The ratio shown in Figure 4 would still be constant and independent of Q but one would calculate a different SLD for ρ_p ($\rho_p = 3.15 \times 10^{10}$ cm^{-2}). While we believe that this assumption is less likely as there is virtually no coherent scattering in the PET-H blank (Figure 2), we have analyzed the data using both assumptions and will show that the results are essentially the same on either basis. It should be noted that the values of ρ_p are quite close to those of the blended samples and so the contribution of the impurity to the total scattering is very small in these samples. The factors multiplying $[(d\Sigma/d\Omega)(Q)]_{100\% PET\text{-}D}$ in eq 4 and 5 range from 0.001 (X = 0.193) to 0.045 (X = 0.39).

Figure 5 shows a Zimm plot of the data for the high molecular weight PET-D. The weight-averaged SANS molecular weight ($M_w = 128 \times 10^3$) agrees with the GPC value ($M_w = 103.6 \times 10^3$) within the overall uncertainty of both determinations. The Zimm plot (Figure 6) for the lower molecular weight PET-D is not as linear as Figure 5, possibly due to differences in the concentration of heterogeneities, leading to uncertainties with the background subtraction. However, the SANS molecular weight (98.8×10^3) is still within 17% of the GPC value (84.7×10^3). Figure 7 shows the R_g and M_w derived from fitting a Debye function to the data of Figure 5. This expression has been shown to give a reasonable description of the SANS patterns for several amorphous polymers$^{3-6}$ although it is not strictly valid for polydisperse samples. The SANS molecular weight (115×10^3) from the Debye fit is closer to the GPC value (103.6×10^3) than that derived from the Zimm fit (128×10^3) and both values are again within the overall uncertainty of the two determinations. While the particular values of SANS M_w shown in Figures 5–7 are higher than the GPC values, they are balanced by data from other samples and the final molecular weights averaged over all samples and fitting procedures are within 12% of the GPC values. The Zimm plots were fitted to

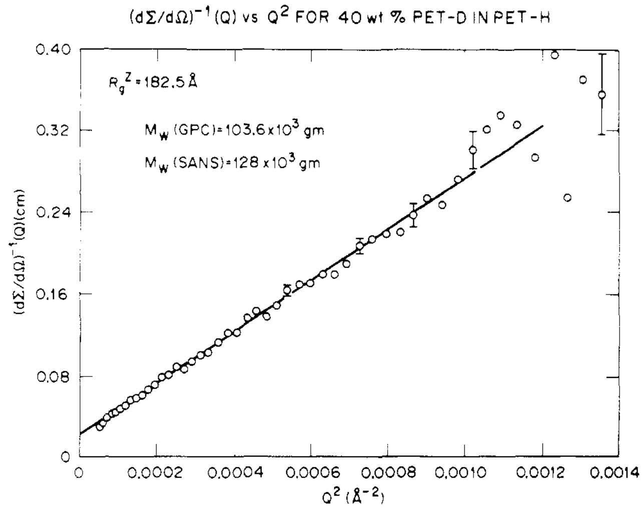

Figure 5. $(d\Sigma/d\Omega)^{-1}(Q)$ vs. Q^2 for radially averaged scattering from 40 wt % PET-D (M_w = 103600) in a PET-H matrix (M_w = 89800). SDD = 12.0 m.

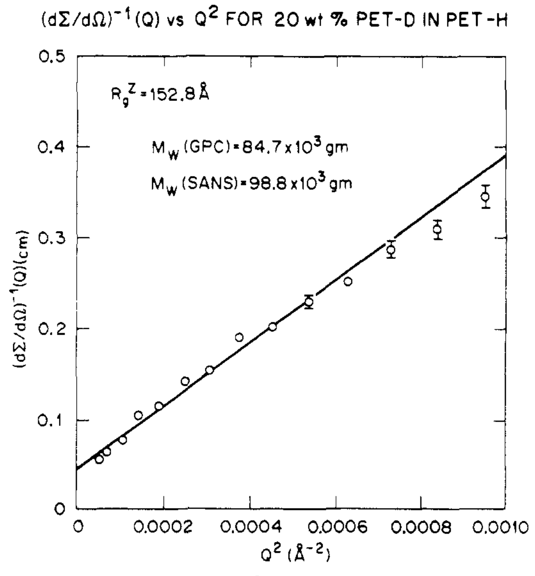

Figure 6. $(d\Sigma/d\Omega)^{-1}(Q)$ vs. Q^2 for radially averaged scattering from 20 wt % PET-D (M_w = 84700) in a PET-H matrix (M_w = 89800). SDD = 4.5 m.

a straight line via the equation[17,18]

$$\left[\left(\frac{d\Sigma}{d\Omega}\right)^{-1}(Q)\right] = \frac{[1 + \Delta w(1 - X)]}{C_N M_{wD}(1 + \Delta w)}\left[1 + \frac{Q^2 R_{\text{gapp}}}{3}\right] \quad (7)$$

where R_{gapp} is an apparent radius of gyration related to the true (z-averaged) radius of the labeled chains R_{gD} by

$$R_{\text{gapp}} = R_{\text{gD}}\left[1 + \frac{X\Delta z}{1 + (1 - X)\Delta w}\right]^{1/2} \quad (8)$$

Δz and Δw depend on the mismatch of the weight-averaged (w) or z-average (z) polymerization indices (N) of the unlabeled (H) and labeled (D) chains as follows:

$$N_{wH} = N_{wD}(1 + \Delta w) \quad (9)$$

$$N_{zH} = N_{zD}(1 + \Delta z) \quad (10)$$

C_N is a constant given by

$$C_N = (a_H - a_D)^2 N_0 X(1 - X)\rho / m_D^2 \quad (11)$$

where a_H and a_D are the coherent scattering lengths of the unlabeled and labeled repeat units, m_D is the mass of a D repeat unit, N_0 is Avogadro's number, and ρ is the density. Where the molecular weight distributions are approximately matched, the volume fraction X may be replaced by the mole fraction.[11]

Using the GPC molecular weight data, we have made corrections to the Zimm fit data for mismatch (eq 7) to yield the weight-averaged M_w and R_g for the D chains, as shown in Table II. These corrections are negligible in some cases, but can be as large as 4%. There do not seem to be any systematic trends within the overall accuracy of the measurements with X, SDD, or the method of background subtraction and so the values of R_g and M_w were averaged over all the points recorded. This gave SANS values of $M_{wD} = 116.3 \times 10^3$ ($M_{wD} = 103.6 \times 10^3$ via GPC) and $M_{wD} = 84.8 \times 10^3$ ($M_{wD} = 84.7 \times 10^3$ via GPC) for sample series A and B, respectively.

In calculating values of the ratio of R_g to $M_w^{1/2}$ we averaged the SANS and GPC molecular weights for each sample series (A and B) and converted the measured z-averaged R_g^z to a weight-averaged R_g^w via the known polydispersity.[19] The magnitude of this correction is 20%. The values of $R_g^w/M_w^{1/2}$ are 0.370 and 0.375 for series A and B, respectively, compared to the unperturbed dimensions of 0.394 (theoretical[20]) or 0.398–0.420 (experimental[20]). Thus, the measured molecular dimensions in PET are again close to those measured in ideal Θ-solvents, as has been found for a range of amorphous polymers. That we obtain essentially unperturbed dimensions in samples with some crystallinity is not surprising, in view of the SANS work on crystallizable polymers. In these studies[6,22,23] it has been shown that R_g is generally very similar in the amorphous and crystalline states.

We have become aware in the course of our work of similar experiments performed by Wu et al.[24] Their specimens were prepared by a melt-pressing technique. High temperatures were avoided in our preparation scheme, since transesterification takes place rapidly in the melt and can complicate interpretation of the scattering curves. We have annealed some of our specimens at elevated temperatures and see significant changes in the scattering behavior after times as short as 10 min. We feel that these changes are at least in part due to transesterification.

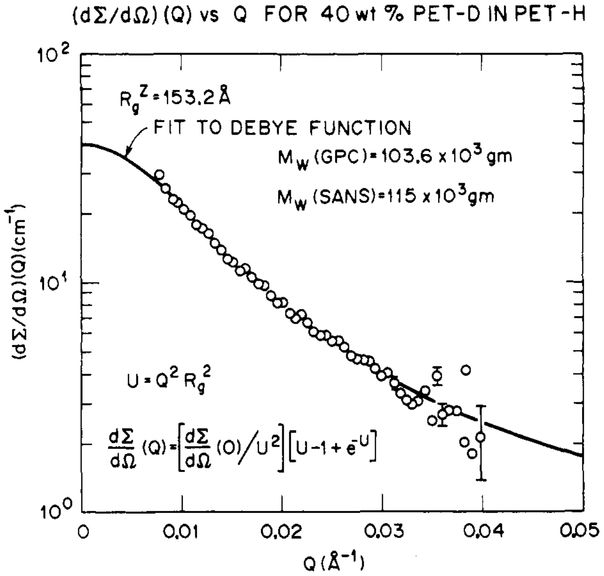

Figure 7. $d\Sigma(Q)/d\Omega$ vs. Q for radially averaged scattering from 40 wt % PET-D (M_w = 103600) in a PET-H matrix (M_w = 89,800) fitted to the Debye function for a random coil.

Acknowledgment. We acknowledge helpful discussions with Dr. D. G. H. Ballard and Dr. G. W. Longman (ICI New Science Group, Runcorn, England), Dr. J. Schelten (KFA, Julich, West Germany), and Dr. R. Ikeda (Du Pont Co., Wilmington) concerning the causes and minimization of background scattering from heterogeneities in PET. In addition, we thank Dr. D. Prevorsek of Allied Chemical for providing the deuterated PET. This research was sponsored by U.S. Army Research Office Grant No. DAAG29-81-C-0187; by the Division of Materials Sciences, and by the National Science Foundation under grant DMR-77 24458, with the U.S. Department of Energy under contract W-7405-eng-26 with the Union Carbide Corp.; and by Oak Ridge Associated Universities.

References and Notes

(1) Kirste, R. G.; Kruse, W. A.; Schelten, J. *J. Makromol. Chem.* **1972**, *162*, 299.
(2) Ballard, D. G. H.; Wignall, G. D.; Schelten, J. *J. Eur. Polym.* **1973**, *J.9*, 965.
(3) Benoit, H.; Cotton, J. P.; Decker, D.; Farnoux, B.; Higgins, J. S.; Jannink, G.; Ober, R.; Picot, C. *Nature (London)* **1973**, *245*, 23.
(4) Wignall, G. D.; Ballard, D. G. H.; Schelten, J. *J. Eur. Polym.* **1974**, *J.10*, 861.
(5) Lieser, G.; Fischer, E. W.; Ibel, K. *J. Polym. Sci.* **1975**, *13*, 39.
(6) Schelten, J.; Ballard, D. G. H.; Wignall, G. D.; Longman, G.; Schmatz, W. *Polymer* **1976**, *17*, 751.
(7) Herschenroeder, P. Thesis, Universität Mainz, Mainz, West Germany, 1978.
(8) Hayashi, H.; Flory, P. J.; Wignall, G. D. *Macromolecules* **1983**, *16*, 1328.
(9) Wignall, G. D. *Trans. Am. Crystallogr. Assoc.* **1983**, *19*, 17.
(10) Ballard, D. G. H.; Schelten, J.; Longman, G. W.; Wignall, G. D., private communication.
(11) Wignall, G. D.; Hendricks, R. W.; Koehler, W. C.; Lin, J. S.; Wai, M. P.; Thomas, E. L. T.; Stein, R. S. *Polymer* **1981**, *22*, 886.
(12) Koehler, W. C.; Hendricks, R. W.; Child, H. R.; King, S. P.; Lin, J. S.; Wignall, G. D. "Scattering Techniques Applied to Supramolecular and Nonequilibrium Systems"; Plenum Press: New York, 1981; p 75.
(13) Hendricks, R. W.; Schelten, J.; Schmatz, W. *Philos. Mag.* **1974**, *30*, 819.
(14) O'Reilly, J.; Teegarden, D. M.; Wignall, G. D., to be submitted for publication.
(15) May, R. P.; Jbel, K.; Haas, J. *J. Appl. Crystallogr.* **1982**, *15*, 15.
(16) Schultz, J. M. "Diffraction for Materials Scientists"; Prentice-Hall: Englewood Cliffs, NJ, 1982; p 236.

(17) Boue, F.; Nierlich, M.; Leibler, L. *Polymer* **1982**, *23*, 19.
(18) Crist, B. W.; Graessley, W. W.; Wignall, G. D. *Polymer* **1982**, *23*, 1561.
(19) Altgelt, K.; Schultz, G. V. *Makromol. Chem.* **1960**, *36*, 209.
(20) Flory, P. J. "Statistical Mechanics of Chain Molecules"; Wiley-Interscience, New York, 1969; pp 191–2.
(21) Wignall, G. D.; Mandelkern, L.; Edwards, C.; Glotin, M. *J. Polym. Sci., Phys. Ed.* **1982**, *20*, 245.
(22) Fisher, E. W.; Stamm, M.; Dettenmaier, M., Herschenroeder, P. *Polym. Prepr., Am. Chem. Soc., Div. Polym. Chem.* **1979**, *20*, 219.
(23) Ballard, D. G. H.; Cheshire, P.; Longman, G. W. *Polymer* **1978**, *19*, 379.
(24) Wu, W. L.; Wise, D.; Zachmann, H. G.; Hahn, D. *Bull. Am. Phys. Soc.* **1984**, *29*, 241.
(25) We have recently performed experiments with newly synthesized PET-D in which the 100% PET-D sample scattering has been reduced by 1 order of magnitude. The value of $R_g/M_w^{1/2}$ obtained with this material is 0.376. As this is almost identical with the average value of 0.373 reported in this paper, we believe that the subtraction method used in our calculations is valid.

Simulation of Small-Angle Neutron Scattering from Microphase-Separated Block Copolymers

R. W. Richards* and J. L. Thomason†

Department of Pure and Applied Chemistry, University of Strathclyde, Glasgow G1 1XL, U.K. *Received October 26, 1983*

ABSTRACT: The small-angle neutron scattering from microphase-separated block copolymers has been simulated on the basis of three major components to the scattered intensity: the single-particle form factor scattering from individual domains, interference function scattering from domain long-range order, and incoherent background scattering. Single-particle form factor scattering may be treated independently of the interference function and special attention has been paid to the use of partly deuterated copolymers and the influence of the orientation of anisometric domains on the scattered intensity. Orientation is found to have a severe influence on the scattered intensity. A comparison is made with experimental data and the agreement is fair. The interference function scattering has been modeled by a paracrystalline lattice modulated by the single-particle form factor scattering from which it is inseparable. Calculation of interference function scattering has been simplified by using a one-dimensional equivalent lattice and adjusting parameters systematically. Comparison with experimental data is reasonable in that the correct positions of the Bragg peaks are obtained, although calculated peaks are narrower and of greater amplitude. The agreement between model and experiment lends support to our conclusion that spherical domains in styrene–isoprene block copolymers are organized on an approximately face-centered cubic lattice. Detector resolution and wavelength distribution are also included while incoherent background is calculated on a relative basis.

Introduction

Microphase separation is a fundamental feature of the solid-state structure of styrene–isoprene block copolymers.[1] Microphase-separated domain morphology has been discussed from a statistical thermodynamics viewpoint and the composition ranges for equilibrium morphologies have been identified.[2-4] Concurrent with theoretical studies have been experimental investigations of block copolymer solid state; for present purposes small-angle scattering studies are of greatest moment. Of particular note is the work of Hashimoto[5-8] dealing with the small-angle X-ray scattering (SAXS) of these copolymers in the solid state and in concentrated solution. Recently, small-angle neutron scattering (SANS) results have been published by us and others.[9-14] The advantages of SANS derive from the prospect of selective labeling; however, major disadvantages are the lower resolution of SANS detectors and the lower signal-to-noise ratio due to incoherent neutron scattering from protons. These two disadvantages assume a greater or lesser importance depending on the scattering vector (**Q**) range investigated. Thus, low resolution broadens Bragg peaks observed at low Q and hinders assignment of long-range structure. At higher Q values, the relatively large background scattering can prevent observation of single-domain scattering and must be carefully accounted for in the analysis of domain–matrix boundaries.

At small scattering vectors, the diffraction patterns from styrene–diene block copolymers are dominated by distinct maxima, Bragg peaks, arising from the long-range order of domains. At higher Q values one or more broad maxima of considerably smaller amplitude may be observed before the intensity decays to a featureless attenuation with increasing Q until an asymptotic intensity is obtained. The broad maxima arise from single-domain scattering while an accelerated attenuation with Q is characteristic of the domain boundary.

Analysis of such diffraction patterns in terms of a structure is often difficult. The Bragg maxima tend to be broad and ill-resolved with absences of expected maxima for particular structures. Single-domain scattering is weak and is weakened still further by the presence of even a modest distribution in domain size. The influence of domain size distribution and a diffuse interface has been discussed by Hashimoto[5-7] especially for spherical domains. Other factors which may be of importance are the domain orientation, for lamellar and cylindrical symmetries, and the level of background scattering.

We report here an attempt to model the SANS from block copolymers using a Fortran package which permits the inclusion of instrumental factors (e.g., wavelength distribution, detector resolution) as well as factors associated with the block copolymers (e.g., domain size, domain spacing, and distributions in these). The approach used is semiempirical in that known scattering laws are used as starting points and the influence of the various factors on them is noted. Finally, the results are compared with experimental data.

Fundamental Equations

A detailed discussion of the equations relating to SANS of block copolymers has been given elsewhere.[10] A brief

---

† Present address: Koninklijke/Shell-Laboratorium, 1003 AA Amsterdam, The Netherlands.

0024-9297/85/2218-0452$01.50/0